Alex *et al. Int J Concr Struct Mater* (2022) 16:40
https://doi.org/10.1186/s40069-022-00531-x

International Journal of Concrete Structures and Materials

RESEARCH Open Access

Flexural Behavior of Low Calcium Fly Ash Based Geopolymer Reinforced Concrete Beam

Alexander Gladwin Alex[1*], Tsegay Gebrehiwet Tewele[1], Zeyneb Kemal[1] and Ramesh Babu Subramanian[2]

Abstract

Pioneering studies have been conducted on alternative cementitious material in the manufacturing of conventional concrete to reduce carbon emission and improve the overall efficacy. However, there are limited studies on eco-friendly materials with low calcium fly ash. This study aims to examine the strength fly ash geopolymer concrete and reduce carbon emission. In this investigation, flexural test is done for conventional and geopolymer concrete (GPC) beam samples after the fulfillment of rest period and 24 h steam curing at 60 °C. The experimental results prove that the initial characteristics of both specimens are almost similar. When GPC specimens reached the service, yield, and failure stages, the load carrying capacity, deflection increased up to 21.5 and 8.75%, respectively and better load bearing capacity, moment resistance, and crack propagation were observed more than in conventional cement. Fresh property test results indicated the achievement of standard workability without the addition of any admixture. Our study show that low calcium based geopolymer can be used as an efficient material for the alternate of cement in cement-based industries with eco-friendly nature.

Keywords: geopolymer concrete, sodium hydroxide, sodium silicate, steam curing, crack propagation, crack width

1 Introduction

The massive production of cement that is 1.3 billion tons every year, is accountable to release 9% of the world's carbon emission and billions of tons of releasing waste and consumed materials (Mehta, 2001; Naik & Moriconi, 2006; Sata et al., 2013). Moreover, the demand of cement is increasing by 10% every year owing to the upswing of infrastructures in many developing countries. In addition, the increasingly old and deteriorated concrete structures requiring urgent repair and rehabilitation. Therefore, the conventional cement compelled researchers to replace fully or partially through byproduct to come up with new sustainable material (Monfardini et al., 2019; Samantasinghar & Singh, 2019). Researchers focus on geo-polymer binders as an alternative so that less energy consumption, reduce carbon emission, with less waste materials can be obtained (Khan et al., 2018). Moreover, recent studies find important pioneer binders of geo-polymer cement from byproduct such as GGBS (Rajendran et al., 2021), rock-based (Ayoub et al., 2021), rice husk ash (RHA) (Shaik et al., 2022), and Fly ash (Chunyang et al., 2022; Colangelo et al., 2018; Fan et al., 2018; Wu et al., 2018). The geo-polymers have better strength, stiffness, and other mechanical properties that make them comparable and superior (Rangan, 2008; Sarker, 2008; Sofi et al., 2007a, 2007b). These types of environmentally friendly binder became popular and has given a chance to replace the conventional cement (Nazari & Sanjayan, 2015).

Construction structures are subjected to harsh environments, including marine systems, bridges, and parking garages, which are exposed to deicing salts and acids causing structural failure (ACI 440.1R-15., 2015). The structural performance of reinforced concrete depends on the bond between the concrete composition elements and structural ties, which is the mechanism to direct the embedded length of reinforcing bar and relates to the

Journal information: ISSN 1976-0485 / eISSN 2234-1315

*Correspondence: gladwinalexa@gmail.com

[1] Department of Building Construction Technology, Ethiopian Technical University, Addis Ababa, Ethiopia
Full list of author information is available at the end of the article

structural performance of load-bearing capacity, crack opening, and spacing (Lloyd et al., 2010; Pop et al., 2013). Considering the bond strength of GPC as one of the structural properties, the understanding of this behavior is critical to eventual development of analysis and design of structural members. Furthermore, the chemical reaction and matrix formation of geo-polymer concrete compared to conventional cement concrete is important and bond properties of geo-polymer concrete should be clearly stated before considering the suitability to replace conventional concrete in reinforced concrete structures. Reliance on conventional bond equations meant for normal concrete could lead to unsafe design that could cause numerous investigations to ascertain the bond behavior of geo-polymer concrete. Due to the importance of bonding properties for structural members, researches have undertaken to evaluate the bond strength between reinforcement and geo-polymer concrete (Sofi et al., 2007a). It was also reported that under-reinforced fly ash-based geo-polymer concrete beams behaved similarly in first cracking load, crack width, load–deflection relationship, flexural stiffness, ultimate load and failure mode compared to conventional reinforced concrete beams subjected to flexural loading (Liew et al., 2016; Dattatreya et al., 2011; Wanchai, 2014; Yost et al., 2013). It is found that the reinforced geo-polymer concrete beams have higher first crack load, mid-span deflection and ultimate load as well as smaller crack width when compared to conventional cement-based concrete beams (Sumajouw & Rangan, 2006; Sumajouw et al., 2005).

The fundamental compositions of GPC have sodium silicate (Na_2SiO_3) and sodium hydroxide (NaOH) is commonly used as an alkaline activator (Hardjito et al., 2004). The combination is alkali-activated solution ($NaOHNa_2SiO_3$) and the alumina-silicate-based materials (Graytee et al., 2018). Likewise, the GPC represented by strong alumina-silicate (Al–SiO_2) polymeric structures results from the generation of alumina and silica by sodium hydroxide (NaOH) or potassium hydroxides (KOH) and sodium silicates (Na_2SiO_3) as an alkaline solution (Kolezynski et al., 2018; Mehta & Siddique, 2017). In addition, the existence of calcium (Ca) compound plays an important role since the calcium ions are able to act as a charge balancing cation in the geo-polymer binder (Davidovits, 1991; Nazari et al., 2014; Okoye et al., 2016). This enhances the overall strength of geo-polymer system as well as improves its microstructure by making it less permeable and more durable (Ankur & Rafat, 2017).

Fly ash geopolymer has important chemical composition, fine size, and easy availability that use hydroxides and sodium or potassium silicate as alkali-activating solutions to form polymerization reactions. The sodium silicate and calcium silicate hydrate alkali-activator enhanced the integrity and denseness of the fly ash geopolymer microstructure; meanwhile, it improve the mechanical properties and formed a three dimensional strong and complex structure (Chunyang et al., 2022). Besides, the material is rich in alumina (Al) and silica (Si) (Khale & Chaudhary, 2007; Komnitsas & Zaharaki, 2007; Mehta & Siddique, 2016; Sharma & Ahmad, 2017); this results in a reaction of calcium aluminosilicate hydrate (C–A–S–H) and sodium aluminosilicate hydrate (N–A–S–H) gel as main alkali-activating that lead to polymeric chains of Si–O–Al–O three-dimensional structure (Duxson et al., 2007; Hardjito & Cheak, 2008). The increment of NaOH concentration in fly ash based GPC specimens improves the compressive strength when heat curing at 60 °C for 48 h (Görhan & Kürklü, 2014; Palomo et al., 1999). The mechanical strength of the GPC system depends on several factors. Amongst, the pH of the activating solution is the primary parameter that controls the compressive strength of a GPC (Khale & Chaudhary, 2007). Moreover, the alkalinity of concrete protects the steel reinforcement (non-prestressed and prestressed) from corrosion, thereby usually resulting in durable and serviceable construction.

There is a limited research on flexural property especially considering shear behavior of shear-critical, similar crack shape, and failure mode (Yost et al., 2013) to predict the ultimate load of the under-reinforced geo-polymer concrete beams. On the other hand, based on IS: 456-2000 (2000), there is fair agreement between predicted and experimental values of the cracking, service, and ultimate moment capacity as well as deflection of the geopolymer concrete beams (Dattatreya et al., 2011). This aspect was noted and researchers introduced equivalent stress block parameters meant for fly ash geo-polymer concrete, which gave good agreement with experimental findings for geo-polymer concrete beams (Prachasaree et al., 2014) and reported that the proposed design parameters could be used with the design procedure (ACI, 2002).

Fly ash is the most important and is extensively used for synthesis of geo-polymer concrete with better mechanical, chemical, thermal and durability properties compared to OPC without fly ash concrete (Walkley et al., 2018). Moreover, it provided better abrasion, corrosion and wear resistance (Chakravarthy et al., 2016; Poojari & Kampilla, 2020). The fly ash geoploymer applicable in heavy construction with up to 50% replacement (Davis et al., 1937) with early strengthen to reduce construction time (Parathi et al., 2021); decreasing water observation with increasing percentage replacement (Naik & Ramme, 1987) and increase compressive strength at later stage with elevated temperature (Ahmed et al., 2020; Ravina & Mehta, 1986). The researches which have been done on

flexural behavior reinforced geo-polymer concrete with combination of different ingredients of geo-polymers and fly ash to compare with the conventional that advanced in able to take more flexural stress (Thakkar et al., 2022), decrease of deflection and increase of first cracking load (Ahmed et al., 2020), ultimate load-carrying capacity and more ductile but higher number of narrow cracks (Marco et al., 2021). The studies reflected that fly ash geo-polymer has superior or similar strength and property of flexural strength and static elastic modulus with the conventional (Singh et al., 2015; Diaz-Loya et al., 2011).

The main parameters affecting the fly ash geo-polymer mixtures are the content of cilium, concentrations of alkaline solutions, and curing method. In GPC, the low calcium fly ash is preferred because high calcium poses the risk of flash setting before casting the elements (Antoni et al., 2020). Thus, fly ash based geopolymer concrete depends on the amount of calcium, which enhance in overall strength, reduce permeation property, and sustainability (Ankur & Rafat, 2017). However, the studies are confined to consider low calcium fly ash without other ingredients, which is very important to improve structural performance and reduce carbon emission. Therefore, this study focused on investigation of strong three-dimensional amorphous alumina silicate network based on low calcium fly ash GPC(with less than 5% of calcium), which the low percentage of calcium fly ash GPCto make eco-friendly material over the conventional concrete. The study investigates the low calcium fly ash based GPC performance for load bearing capacity, deflection, crack propagation, and moment resistance.

2 Materials and Methodology

2.1 Fly Ash

For the production of geopolymer concrete, low calcium fly ash has been used. Aluminum oxide and silica oxide together accounted for 80% of the total mass of fly ash. The proportion of silica, on the other hand, is twice that of alumina. Iron oxides were found in concentrations ranging from 10 to 20% by mass with less than 2% of carbon content. The calcium oxide level was extremely low, which is 1.26% the overall mass (ASTM Class F). Low calcium fly ash from the Mettur thermal power plant was used to make GPC. The SEM analysis shows that the majority of the particles are in spherical shape with different size, meanwhile porous micro phase structures are also found in Mettur Fly ash when observed in-depth (Fig. 1).The chemical composition was measured by EDS (Fig. 2) and Table 1 represents the concentration of major elements.

2.2 Aggregates

Single source crushed hard blue granite with a maximum size of 19 mm with no dust or impurities were used as the coarse aggregate. Table 2 shows the fine and coarse aggregate parameters obtained using IS 2386-4 (IS, 1963). The particle size distribution (PSD) of the aggregates was

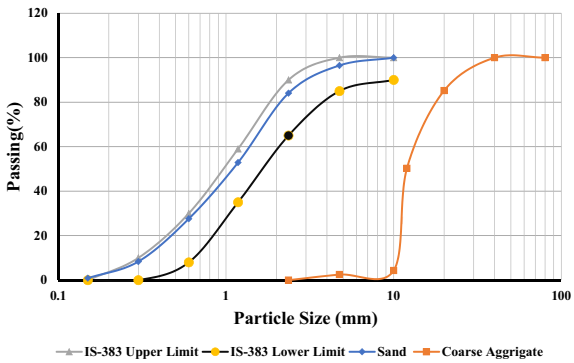

Fig. 2 Particle size distribution of aggregates.

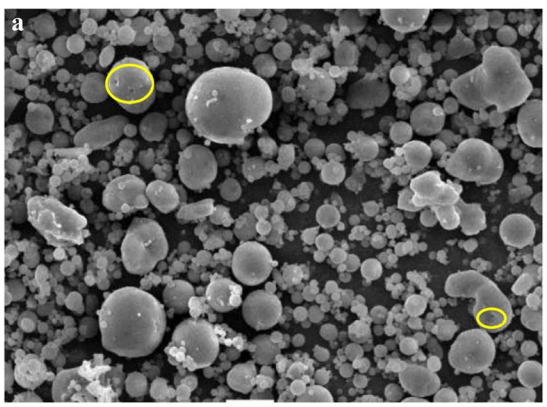

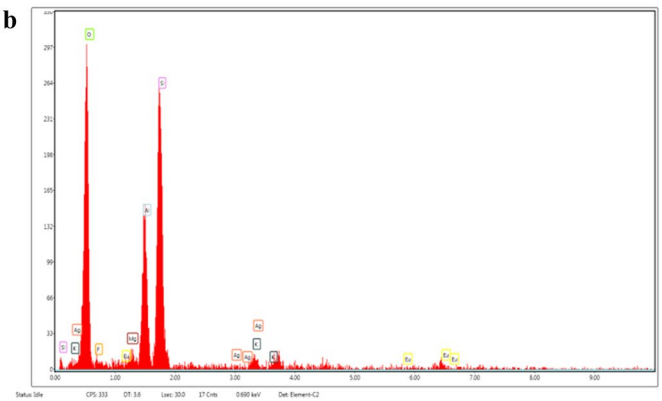

Fig. 1 **a** SEM photograph of fly ash. **b** EDX result of fly ash.

Table 1 Concentrations of major elements (%) in Mettur fly ash.

Compound	SiO_2	Al_2O_3	Fe_2O_3	CaO	Na_2O	K_2O	TiO_2	MgO	P_2O_5	SO3	LoI
% in mass	52.57	26.69	11.32	1.26	0.46	0.79	1.53	0.89	1.57	1.64	1.28

Table 2 Physical properties of aggregates.

Sl. no.	Characteristics	Coarse aggregate	Fine aggregate
1	Specific gravity	2.67	2.68
2	Bulk density loose(kg/l)	1.48 kg/m^3	1.49 kg/m^3
3	Fineness modulus	2.21	2.77
4	Water absorption	0.65	Nil
5	Grading zone	Zone-II	Zone-II

determined using IS 383 (IS, 1970), as shown in Fig. 2, fits within Zone-II suggested limits. Natural river sand with no contaminants was used as the fine aggregate.

2.3 Alkaline Liquid

In this study, the alkaline liquid is prepared by mixing of sodium hydroxide solution (8 M) and sodium silicate. Commercially available sodium hydroxide pellets (97–98 percent purity) were used. The molecular weight of sodium hydroxide is 40, to prepare an 8 M solution, $8 \times 40 = 320$ g of Sodium Hydroxide was dissolved in 1000 ml of water. The commercially available sodium silicate (Na_2SiO_3) with 8 M sodium hydroxide (NaOH) by mass ratio of 2.5 was used. The prepared solution was allowed to cool for 24 h, to full fill the polymerization.

2.4 Control and Geo-Polymer Concrete Preparation

For making control concrete, Coromandel OPC cement of 43 grade conforming IS 8112 with initial and final setting time of 140 min and 355 min, respectively was used. The nominal mix ratio (1:1.5:3) of M20 grade, which is the minimum grade of concrete as per IS 456-2000 was used in this study, W/C ratio of 0.5 was maintained. For GPC low calcium fly ash was used as a binder and alkaline liquid to binder ration of 0.45 was maintained without adding any type of super-plasticizers. The conventional Portland cement concrete mixing technique was used for making GPC. The fly ash and fine aggregates are mixed well together in a pan mixer for 3 min. The surface dried coarse aggregates were added and mixed until the coarse aggregates are uniformly distributed throughout the mix. Alkaline solution was added and entire batch was mixed well for three to 4 min. The workability of the fresh concrete was measured by means of the conventional slump test, and the slump measured in the control and 8 M of Na OH concentration concrete was 180 and 175 mm respectively. The constituents of control and GPC of 8 M NaOH for M20 grade concrete was shown in Table 3.

Table 3 Mix proportions of control and geopolymer concrete (kg/m^3).

Beam designation	CB	GPC
Grade of concrete	M20	M20
Cement	383	–
Flay ash	–	437
Water to binder ratio	0.5	–
Na_2SiO_3/NaOH	–	17.93
(Na_2SiO_3/NaOH)/fly ash		0.45
Water	191.6	38.12
Fine aggregate	652	652
Coarse aggregate	1308	1308
Curing	28 days water	60 °C at 24 h
Slump value (mm)	145	132

2.5 Casting and Curing

The prepared concrete was cast in cube mold specimen size of 100 × 100 × 100 mm, the specimen for cylinder size is 100 × 300 mm, the specimen for beam was 100 × 100 × 500 mm and the size of specimen was 125 × 250 × 3200 mm. Compaction of fresh concrete in the cube and cylinder steel molds was achieved by applying sixty manual strokes per layer in three equal layers, followed by compaction on a vibration table for ten seconds. The beam steel molds are compacted by using needle vibrator for 10–15 s in one location. After casting, the specimens were kept in the room for one day at room temperature for the requirement of rest period. Completion of rest period for the specimens were covered using vacuum bagging film. Curing at elevated temperature was done at 60 °C in a steam curing chamber for 24 h. A boiler was used to generate the steam at a specified temperature. Curing process in the steam–curing chamber is represented in Fig. 3a, b.

2.6 Experimental Investigation

From the total specimen of 18, 12 of the specimens are used for preliminary investigation. The remaining six of the beam specimens having the size of $125 \times 250 \times 3200$ mm are used in experimental program. Three beams were used as control cement concrete and

Fig. 3 **a** Control panel. **b** Steam chamber.

three beams were used as GPC beams. The beams were designed under reinforced sections. It was reinforced with 2 Nos of 12 Φ at Tensile bar and 2 Nos of 10 Φ at compressive zone with the clear cover of 20 mm. Eight Φ bars was used for two legged stirrups at 150 mm C/C. The grade of steel used was Fe 415. The average yield strength of 12, 10, 8 mm steel bars (HYSD) was found to be 435.6 N/mm^2. The control beams were casted using M20 grade with W/C of 0.5 as per IS 456-2000 OPC. Natural River sand and crushed hard blue granite of maximum size 20 mm aggregate were used for control mix. The elastic modulus of GPC was found to be 2.21×10^4 N/mm^2 and the Poisson's ratio was 0.12. The control and geo-polymer beams were designated as Control Beam (CB-1, CB-2, CB-3) and Geo-polymer Concrete (GPC-1, GPC-2, GPC-3). Companion cubes and cylinders of standard size were also casted with beams and tested.

2.7 Test Setup

The specimen was mounted on a beam testing frame of 500 kN capacity. The beams were simply supported over the span of 3000 mm and subjected to two concentrated loads placed symmetrically on the span. The distance between two-point loads was 1000 mm. The load was applied 500 mm away from the center of both sides towards support. The dial gauges of 0.001 mm least count was used for measuring the deflections under the loading points and mid-span of beam. The dial gauge readings were recorded at different loads. The strain in concrete was measured using demec gauge. An automatic data acquisition unit was used to collect the data during the test. Linear variable data transformers (LVDT's) were placed at mid-span under the loading point of beam. The load was applied at the regular interval of 2.5 kN. The first crack load was obtained by visual examination. The test set up of beams is shown in Fig. 4a, b

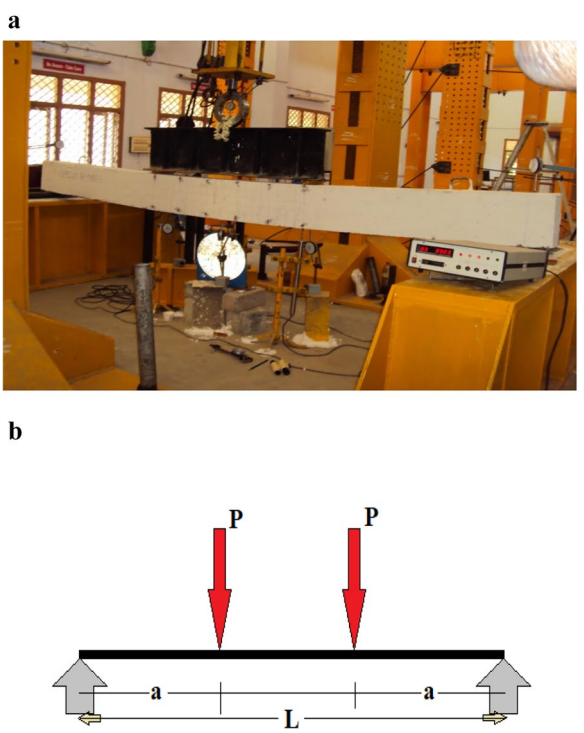

Fig. 4 **a** Beam testing set up. **b** Loading arrangement.

3 Result and Discussion

3.1 Crack and Failure Patterns

The crack and failure patterns of CB and GPC specimens are almost similar. The initial cracks were found in the constant moment region of both beam specimens. The development of cracks in each GPC was almost same and the crack usually occurred with slight noise. In the

CB beam, however, the cracks penetrated farther into the compressive zone than in the GPC beam. New cracks emerged after the initial crack, and the widths of the existing cracks widened with the load in both the CB and GPC beams. The cracks were mostly distributed at the longitudinal point and mid-span. At the same time, the crack width also increased gradually more than 1.5 mm for CB and 1 mm for GPC. Less cracks occurred in the GPC beams than in the CB beams at yield and maximum loads. GPC showed a 16.66 kN average first crack load, which was slightly greater than CB's 13.66 kN. The first crack usually ran through 30–70% of the beam height for CB and 25–60% for GPC. The crack extended upward along the beam upon increase in load. The CB members' typical failure was caused by a sudden high amount of crushing of the concrete in the compressive zone, whereas the GPC beams' typical failure was caused by less amount of crushing in compressive zone. The compressive zone of CB and GPC is shown in Fig. 5a, b.

3.2 Load and Deflection Curves

The load and deflection curves of CB and GPC are shown in Fig. 6a, b. In initial crack stage, CB showed an average deflection of 0.753 mm with 3.00 kN load less than GPC, while a deflection of 1.053 mm was observed in GPC with an additional load of 3.00 kN. In service stage, deflection of CB and GPC were identical. But the average load carrying capacity was increased up to 15.74% for GPC. In the yield stage, GPC specimen showed average load carrying capacity of 21.57% with the deflection of 12.01% when compared to CB. In ultimate stage, GPC exhibited more deflection compared to CB. However, in flexural mode all the beam specimens failed. In GPC specimens, the average load carrying capacity was increased to 21.06% with a raise of 8.74% deflection compared to CB. Load deflection behavior of both CB and

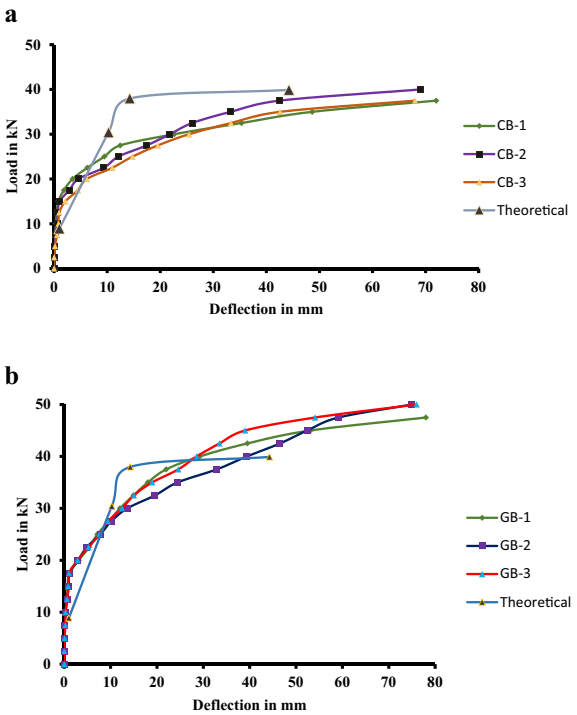

Fig. 6 **a** Mid span deflection of CB. **b** Mid span deflection of GPC.

GPC were compared with theoretical values and represented in Fig. 6a and b; the theoretical value is calculated using the following equation.

$$\delta_{\max} = \frac{Pa}{24EI}(3l^2 - 4a^2)$$

where, P = Load (kN), a = distance from point (m), l = effective length of beam (m), E—Young's modulus (N/m^2),and I—moment of inertia (N/mm^2).

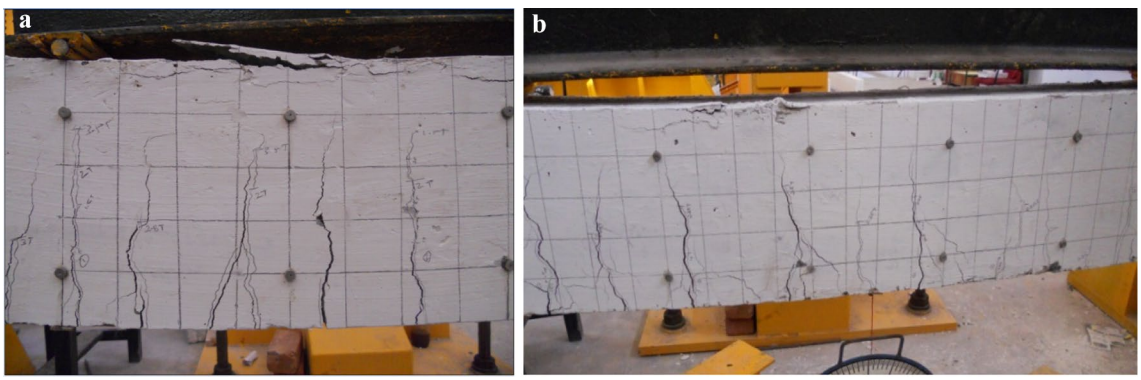

Fig. 5 **a** Crack pattern of CB. **b** Crack pattern of GPC.

3.3 Moment Curvature Relation

The strength, stiffness and ductility properties of the cross-section of the structural member under the effect of bending can be defined by moment curvature relationship. For the same load level, GPC showed a large deflection than CB without crack formation indicating that GPC has a good ductile nature rather than CB at the same reinforcement ratio. Further, the mid-span deflection of GPC was decreased with an increase in ultimate bending moment (M_u) for the same load level. The observed properties may be due to the ultimate load bearing capacity of the GPC was shared by the tensile reinforcement and concrete. When the load bearing capacity of the tensile reinforcement was constant, the bearing capacity of concrete increased and M_u of GPC also increased. Theoretical curvature value was calculated according to the following equation:

$$\varphi = \frac{M}{EI}$$

where φ—curvature (rad/mm); M—bending moment (N-m); E—Young's modulus; I—moment of inertia (N/mm^2).

The theoretical and experimental moment curvature relationships are shown in Fig. 7.

3.4 Characteristics Process

The concrete grade and reinforcement ratio are same, and all the six beam specimens exhibited the failure characteristics of under reinforced beams and the deformation characters could be divided into 4 stages (Fig. 8).

3.4.1 Stage 1

Beam cracking that occurs under loading condition is regarded as the elastic stage (Stage 1). From the results it is observed that at the initial stage of loading, the bending moment (M_u) is very small. At the elastic stage the mid-span deflection bending moment curves increases linearly. Under the loading condition, both CB and GPC exhibit almost similar characteristics. When M reached about M_{cr} the concrete strain of GPC in the tension zone reached the concrete ultimate tensile strain. When the beam undergoes large plastic deformation, small cracks appear in tensile zone.

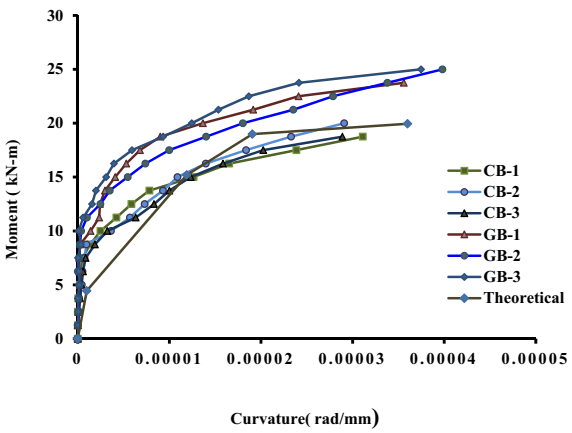

Fig. 7 Moment curvature of CB and GPC.

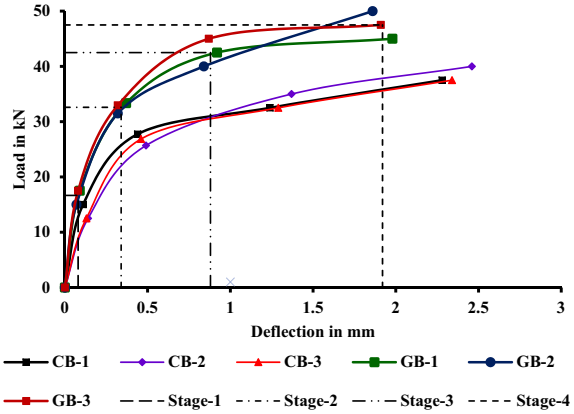

Fig. 8 Deformation characters of CB and GPC.

3.4.2 Stage 2

Upon continuous increase in load, first crack appears in the concrete beam in pure bending section when M reaches M_{cr}. As the load is increased, first crack occurred at the section of the concrete that had a small f_t within the pure bending section or near the loading point. The crack ran through 25–65% of beam height. The first crack of GPC was shorter than CB, which could be due to the higher bonding strength of GPC binder compared to the control mix of CB. The cracks showed crack maximum width of 1.98 mm and 2.46 mm for GPC and CB respectively. When M_u reaches 85–90% of M_u, the bar at tensile zone starts yielding resulting in the end of stage.

3.4.3 Stage 3

After the yielding of steel bar stress (σ) of the reinforcement remains constant or slightly increased, indicating failure stage. The increment of M was balanced by the addition of arm force and an extension in crack was observed at this stage. Further, deflection and crack width (W) were also found to be promptly increased at this stage. The point where the reinforcement was yielded in the pure bending section, a principal crack of large width was observed.

Table 4 The basic parameter and bearing capacity of CB and GPC.

Beam designation	f_{cu} (Mpa)	f_c (Mpa)	f_t (Mpa)	ρ (%)	M_{cr} (kN m) (theoretical)	M_{cr} (kN m) (experimental)	M_u (kN m) (theoretical)	M_u (kN m) (experimental)	M_{cr}/M_u	f_{max} (mm)	W_s (mm)	l_m (mm)
CB-1	23.60	19.82	2.80	0.807	4.45	4.49	19.95	20.20	0.22	72	2.28	154.3
CB-1	22.80	19.38	2.45	0.807		3.93		20.15	0.19	69	2.46	156.7
CB-1	24.10	20.13	2.90	0.807		4.66		20.22	0.23	68	2.34	152.7
GPC-1	25.40	21.33	3.06	0.807		4.91		20.29	0.24	78	1.98	131.8
GPC-2	27.60	23.21	3.40	0.807		5.46		20.38	0.26	75	1.86	132.4
GPC-3	26.13	20.86	3.15	0.807		5.06		20.32	0.25	76	1.91	132.9

f_y is yield strength of steel, f_u is the tensile strength of steel, f_{cu} is cube compressive strength, f_c is the compressive strength of prism and f_t is the tensile strength of concrete, M_{cr} is the cracking bending moment, M_u is the ultimate bending moment, f_{max} maximum deflection, W_s is the maximum crack width, l_m is the average crack space.

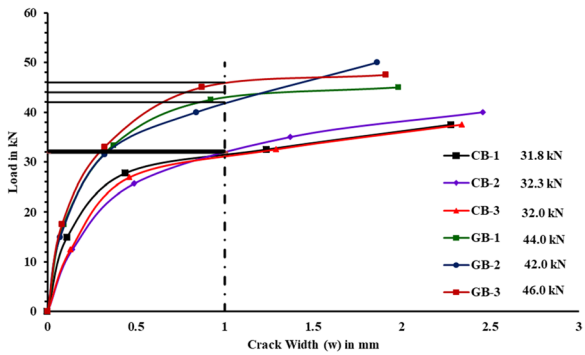

Fig. 9 Crack width of CB and GPC.

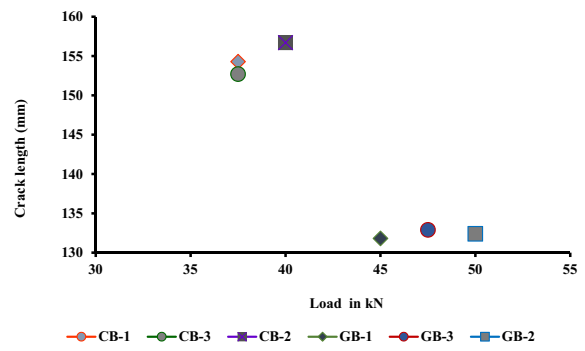

Fig. 10 The average crack space of CB and GPC.

3.4.4 Stage 4

When the load was continuously increased, in a certain area on both sides of principal crack on the top of the beam, the compressive zone concrete produced a large plastic deformation forming a concentrated plastic deformation zone. Upon crushing of concrete in the compression zone, the deflection of the beam increased rapidly resulting in the failure of beam.

3.5 Bearing Capacity Analysis

At same load levels, the ratio of cracking bending moment (M_{cr}) with ultimate moment (M_u) was increased, indicating that the bearing capacity of the GPC was higher than CB. It is also observed that M_{cr} and M_u of the GPC was high rather than CB, denoting before cracking, the tensile stress was mainly commenced by concrete and it had a very closer relation to f_t of GPC. The theoretical M_{cr} and M_u values are validated, and the bearing capacity results of CB and GPC were shown in Table 4.

3.6 Crack Width

The crack width (w) increases with increase in load. However, at the beginning stage of loading, crack width (w) increases slowly. As the load reaches closer to the ultimate stage, crack width (w) increases rapidly until the beam fails. The relationship between load and crack were similar to the trend of logarithmic function during the development of crack. When $W=1$ mm, load at the level of CB-1, CB-2, CB-3 was 31.8 kN, 32.3 kN, 32.0 kN and GPC-1, GPC-2, GPC-3 was 44 kN, 42 kN, and 46 kN, respectively (Fig. 9). In addition, it is also observed that when the reinforcement ratio (ρ) is constant for both cases, crack width (w) development and strength of concrete are interrelated. Further, the increase of strength in concrete reduces the crack development which might be because of the higher binding strength of the three-dimensional polymeric chain of Si–O–Al–O bond in the geo-polymer compared to OPC cement paste as well as the amorphous structure of the bond.

3.7 Crack Space

Control concrete showed lesser space between cracks compared to GPC specimens, which is mainly due to the interlock between the binder and aggregates of concrete indicating the interface bond strength of GPC was higher than CB. Fig. 10 shows the average crack space (l_m) of both control and GPC specimens. The basic parameters of CB and GPC were showed in Table 4.

4 Conclusion

(1) The average first cracking load of geo-polymer beam was around 22% higher than control concrete and it gives higher deflection, indicating the binding between inner matrixes of GPC mix has more bond strength compared to conventional concrete.
(2) In the service stage and yield stage, GPC exhibited better performance in the aspects of load carrying and deflection compared to control concrete, which shows GPC have more ductility compared to conventional concrete.
(3) The crack width increased gradually with increase in load. In the case of GPC, crack width increased slowly up to service stage. However, when it reached the ultimate stage, it increased rapidly. The average spacing between cracks in GPC is more when compared to conventional concrete.
(4) The application of low calcium fly ash-based GPC was suggested effectively in the replacement of conventional concrete, as it shows better performance and reduces environmental issues.

Acknowledgements
The authors would like to acknowledge Professor, Dr. S. Thirugnanasambandam for advising this project and the help from the concrete laboratory at

Annamalai University for permission of performing the experiments and imaging.

Author contributions
AGA: conceptualizations, formal analysis, investigation, design, experimentation, writing original/final draft, writing—review/editing visualization supervision and project administration. TG: writing—review/editing, formal analysis. ZK: writing—review/editing, RB: formal analysis. All authors read and approved the final manuscript.

Authors' information
Alexander Gladwin Alex is Assistant Professor of Building construction Technology Department, Ethiopian Technical University, Addis Ababa, Ethiopia. He received PhD from Annamalai University, India in 2018 and his research is on the Geo-polymer Concrete. Tsagye is Assistant Professor of Building construction Technology Department, Ethiopian Technical University, Addis Ababa, Ethiopia. He received his PhD from University, China and his research is sustainable concrete and Construction Management. Zaynabkamel Kamel is of Building construction Technology Department, Ethiopian Technical University, Addis Ababa, Ethiopia. Her research interest cement and alternate materials. Ramesh Babu Subramanian is a Professor in Department of Mechanical Engineering in NallaMalla Reddy Engineering College, Hyderabad, India.

Funding
There has been no officially assigned funding regarding this manuscript and it is a result of self-motivated work.

Availability of data and materials
The datasets generated during and/or analyzed during the current study are available from the corresponding author on reasonable request.

Declarations

Competing interests
The authors wish to confirm that there are no known competing interests associated with this publication.

Author details
[1]Department of Building Construction Technology, Ethiopian Technical University, Addis Ababa, Ethiopia. [2]Department of Mechanical Engineering, NallaMalla Reddy Engineering College, Hyderabad, India.

Received: 19 May 2021 Accepted: 19 April 2022
Published online: 02 August 2022

References

ACI 440.1R-15. (2015). *Guide for the design and construction of concrete reinforced with fiber reinforced polymers (FRP) bars. ACI Committee 440.* Farmington Hills: American Concrete Institute.

ACI (American concrete institute). (2002). *Building code requirements for structural concrete (ACI 318-05)*. Farmington Hills: American Concrete Institute.

Ahmed, H., Jaf, D., & Yaseen, S. (2020). Flexural capacity and behaviour of geopolymer concrete beams reinforced with glass fibre-reinforced polymer bars. *International Journal of Concrete Structures and Materials*. https://doi.org/10.1186/s40069-019-0389-1

Ankur, M., & Rafat, S. (2017). Properties of low-calcium fly ash based geopolymer concrete incorporating OPC as partial replacement of fly ash. *Construction and Building Materials*. https://doi.org/10.1016/j.conbuildmat.2017.06.067

Antoni, A., Purwantoro, A., Suyanto, W., et al. (2020). Fresh and hardened properties of high calcium fly ash-based geopolymer matrix with high dosage of borax. *Iranian Journal of Science and Technology, Transactions of Civil Engineering, 44*, 535–543. https://doi.org/10.1007/s40996-019-00330-7

Ayoub, A., Abdellah, B., Abdelilah, B., Thamer, A., Iz-Eddine, E., Mohammed, A., Hamid, E., Yassine, E., & FaizUddin, A. (2021). Effect of acidic volcanic perlite rock on physio-mechanical properties and microstructure of natural pozzolan based geopolymers. *Case Studies in Construction Materials, 15*, 2214–5095. https://doi.org/10.1016/j.cscm.2021.e00712

Chakravarthy, R., Venkatesan, S., & Patnaikuni, I. (2016). Mechanical properties of high volume fly ash concrete reinforced with hybrid fibers. *Advances in Materials Science and Engineering*. https://doi.org/10.1155/2016/1638419

Chunyang, L., Qingping, W., Yuxin, L., Tingting, X., Qingbo, Y., & Shuai, C. (2022). Influence of new organic alkali activators on microstructure and strength of fly ash geopolymer. *Ceramics International*. https://doi.org/10.1016/j.ceramint.2022.01.109

Colangelo, F., Roviello, G., Ricciotti, L., Ferrandiz-Mas, V., Messina, F., Ferone, C., Tarallo, O., Cioffi, R., & Cheeseman, C. (2018). Mechanical and thermal properties of lightweight geo-polymer composites. *Cement and Concrete Composites, 86*, 266–272. https://doi.org/10.1016/j.cemconcomp.2017.11.016

Ravina, D., & Mehta, P.K. (1986). Properties of fresh concrete containing large amounts of fly ash. *Cement and Concrete Research, 16*(2), 227–238. https://doi.org/10.1016/0008-8846(86)90139-0

Dattatreya, J., Rajamane, N., Sabitha, D., Ambily, P., & Nataraja, M. (2011). Flexural behaviour of reinforced geopolymer concrete beams. *International Journal of Civil and Structural Engineering, 2*(1), 138–159. https://doi.org/10.1109/ICEEOT.2016.7755347

Davidovits, J. (1991). Geopolymers geopolymers inorganic polymeric new materials. *Journal of Thermal Analysis, 37*, 1633–1656. https://doi.org/10.1007/bf01912193

Davis, R., Carlson, R., Kelly, J., & Davis, A. (1937). Properties of cements and concretes containing fly ash. *Journal Proceedings, 33*(1937), 577–612.

Diaz-Loya, E., Allouche, E., & Vaidya, S. (2011). Mechanical properties of fly ash based geopolymer concrete. *ACI Materials Journal, 108*(3), 300–306.

Duxson, P., Provis, J., Lukey, G., & VanDeventer, J. (2007). The role of inorganic polymer technology in the development of 'green concrete.' *Cement and Concrete Research, 37*(12), 1590–1597. https://doi.org/10.1016/j.cemconres.2007.08.018

Fan, F., Liu, Z., Xu, G., Peng, H., & Cai, C. (2018). Mechanical and thermal properties of fly ash based geo-polymers. *Construction and Building Materials, 160*, 66–81. https://doi.org/10.1016/j.conbuildmat.2017.11.023

Görhan, G., & Kürklü, G. (2014). The influence of the NaOH solution on the properties of the fly ash-based geopolymer mortar cured at different temperatures. *Composites, Part b: Engineering, 58*, 371–377. https://doi.org/10.1016/j.compositesb.2013.10.082

Graytee, J., Sanjayan, A., & Nazari,. (2018). Development of a high strength fly ash based geopolymer in short time by using microwave curing. *Ceramics International, 44*, 8216–8222. https://doi.org/10.1016/J.CERAMINT.2018.02.001

Hardjito, D., & Cheak, C. (2008). Strength and setting times of low calcium fly ash based geopolymer mortar. *Modern Applied Science, 2*(4), 3–11. https://doi.org/10.5539/mas.v2n4p3

Hardjito, D., Wallah, S., Sumajouw, D., & Rangan, B. (2004). On the development of fly ash- based geopolymer concrete. *ACI Materials Journal, 101*, 467–472. https://doi.org/10.14359/13485

IS 383-1970, Indian Standard. (1970). *Specification of course and fine aggregates from natural sources for concrete*. New Delhi: BIS.

IS: 456-2000, Indian Standard. (2000). *Plain and reinforced concrete—code of practice*. New Delhi: BIS.

IS 2386(part-I), Indian Standard. (1963). *Methods of test for aggregate for concrete*. New Delhi: BIS.

Khale, D., & Chaudhary, R. (2007). Mechanism of geopolymerization and factors influencing its development: A review. *Journal of Materials Science, 42*(3), 729–746. https://doi.org/10.1007/s10853-006-0401-4

Khan, M., Zafar, A., Farooq, F., Javed, M., Alyousef, R., Alabduljabbar, H., & Khan, M. (2018). Geopolymer concrete compressive strength via artificial neural network, adaptive neuro fuzzy interface system, and gene expression programming with K-fold cross validation. *Frontiers in Materials*. https://doi.org/10.3389/fmats.2021.621163

Kolezynski, A., Król, M., & Żychowicz, M. (2018). The structure of geopolymers Theoretical studies. *Journal of Molecular Structure, 1163*, 465–471. https://doi.org/10.1016/j.molstruc.2018.03.033

Komnitsas, K., & Zaharaki, D. (2007). Geopolymerisation: a review and prospects for the minerals industry. *Mineral Engineering, 20*(14), 1261–1277. https://doi.org/10.1016/j.mineng.2007.07.011

Liew, Y., Heah, C., & Kamarudin, H. (2016). Structure and properties of clay-based geopolymer cements: a review. *Progress in Materials Science, 83*, 595–629. https://doi.org/10.1016/j.pmatsci.2016.08.002

Lloyd, N., Rangan, B., Zachar, J., Claisse, P., Naik, T., & Ganjian, G. (2010). Geopolymer concrete with fly ash. *Second international conference on sustainable construction materials and technologies* (Vol. 3, pp. 1493–1504). Ancona: UWM Centre for By-products Utilization.

Marco, V., Matteo, S., & Abbas, S. (2021). Geopolymers vs. cement matrix materials: How nanofiller can help a sustainability approach for smart. *Nanomaterials, 11*(8), 2007. https://doi.org/10.3390/nano11082007

Mehta, P. (2001). Reducing the environmental impact of concrete. *Concrete International, 23*(10), 61–66.

Mehta, A., & Siddique, R. (2016). An overview of geopolymers derived from industrial byproducts. *Construction and Building Materials, 127*(2016), 183–198. https://doi.org/10.1016/j.conbuildmat.2016.09.136

Mehta, A., & Siddique, R. (2017). Sulfuric acid resistance of fly ash based geopolymer concrete. *Construction and Building Materials, 146*, 136–143. https://doi.org/10.1016/j.conbuildmat.2017.04.077

Monfardini, L., Facconi, L., & Minelli, F. (2019). Experimental tests on fiber-reinforced alkali-activated concrete beams under flexure: some considerations on the behavior at ultimate and serviceability conditions. *Materials, 12*(20), 3356. https://doi.org/10.3390/ma12203356

Naik, T., & Moriconi, G. (2006). *Environmental-friendly durable concrete made with recycled materials for sustainable concrete construction*. Milwaukee: University of Wisconsin.

Naik, T., & Ramme, B. (1987). *Setting and hardening of high fly ash content concrete* (Vol. 1, pp. 161–1620). Atlanta: Proceedings of the Eighth International Ash Utilization Symposium.

Nazari, A., & Sanjayan, J. (2015). Hybrid effects of alumina and silica nanoparticles on water absorption of geopolymers: application of Taguchi approach. *Measurement, 60*, 240–246. https://doi.org/10.1016/j.measurement.2014.10.004

Nazari, A., Torgal, F., Cevik, A., & Sanjayan, J. (2014). Compressive strength of tungsten mine waste-and metakaolin-based geopolymers. *Ceramics International, 40*, 6053–6062. https://doi.org/10.1016/j.ceramint.2013.11.055

Okoye, F., Durgaprasad, J., & Singh, N. (2016). Effect of silica fume on the mechanical properties of fly ash based-geopolymer concrete. *Ceramics International, 42*, 3000–3006. https://doi.org/10.1016/j.ceramint.2015.10.084

Palomo, A., Grutzeck, M., & Blanco, M. (1999). Alkali-activated fly ashes: a cement for the future. *Cement and Concrete Research, 29*, 1323–1329. https://doi.org/10.1016/S0008-8846(98)00243-9

Parathi, S., Nagarajan, P., & Pallikkara, S. (2021). Ecofriendly geopolymer concrete: a comprehensive review. *Clean Technologies and Environmental Policy, 23*, 1701–1713. https://doi.org/10.1007/s10098-021-02085-0

Poojari, Y., & Kampilla, V. (2020). Strength behavior analysis of fiber reinforced fly ash concrete. *Materials Today*. https://doi.org/10.1016/j.matpr.2020.10.027

Pop, I., DeSchutter, G., Desnerck, P., & Onet, T. (2013). Bond between powder type self-compacting concrete and steel reinforcement. *Construction and Building Materials, 41*, 824–833. https://doi.org/10.1016/j.conbuildmat.2012.12.029

Prachasaree, W., Limkatanyu, S., Hawa, A., & Samakrattakit, A. (2014). Development of equivalent stress block parameters for fly-ash-based geopolymer concrete. *Arabian Journal for Science and Engineering, 39*(12), 8549–8558. https://doi.org/10.1007/s13369-014-1447-2

Rajendran, R., Narasimharao, B., Preethi, P., Mohammed, S., Naveen, D., Prem, A., & Pratheba, S. (2021). Strength analysis of geo-polymer concrete based on GGBS/rise husk and p-sand. *Materials Today: Proceedings*. https://doi.org/10.1016/j.matpr.2021.08.126

Rangan, B. (2008). *Fly ash based geopolymer concrete. Research report GC4*. Perth: Curtin University of Technology.

Samantasinghar, S., & Singh, S. (2019). Fresh and hardened properties of fly ash-slag blended geopolymer paste and mortar. *International Journal of Concrete Structures and Materials, 13*, 47. https://doi.org/10.1186/s40069-019-0360-1

Sarker, P. (2008). A constitutive model for fly ash-based geopolymer concrete. *Architecture Civil Engineering Environment, 1*, 113–120.

Sata, V., Wongsa, A., & Chindaprasirt, P. (2013). Properties of pervious geopolymer concrete using recycled aggregates. *Construction and Building Materials, 42*, 33–39. https://doi.org/10.1016/j.conbuildmat.2012.12.046

Shaik, N., Dushyanth, V., Nabil, H., & Mohd, M. (2022). Strength and durability properties of geopolymer paver blocks made with fly ash and brick kiln rice husk ash. *Case Studies in Construction Materials, 16*, 2214–5095. https://doi.org/10.1016/j.cscm.2021.e00800

Sharma, A., & Ahmad, J. (2017). Factors affecting compressive strength of geopolymer concrete—a review. *International Research Journal of Engineering and Technology, 4*, 2026–2031.

Singh, B., Ishwarya, G., Gupta, M., & Bhattacharyya, S. (2015). Geo-polymer concrete: a review of some recent developments. *Construction and Building Materials, 85*, 78–90. https://doi.org/10.1016/j.conbuildmat.2015.03.036

Sofi, M., VanDeventer, J., Mendis, P., & Lukey, G. (2007a). Engineering properties of inorganic polymer concretes (IPCs). *Cement and Concrete Research, 37*, 251–257. https://doi.org/10.1016/j.cemconres.2006.10.008

Sofi, M., VanDeventer, J., Mendis, P., & Lukey, G. (2007b). Bond performance of reinforcing bars in inorganic polymer concrete (IPC). *Journal of Materials Science, 42*, 3107–3116. https://doi.org/10.1007/s10853-006-0534-5

Sumajouw, D., & Rangan, B. (2006). *Low-calcium fly ash-based geopolymer concrete: Reinforced beams and columns. Research report GC 3*. Perth: Curtin University of Technology.

Sumajouw, D., Hardjito, D., Wallah, S., & Rangan, B. (2005). *Behaviour and strength of reinforced fly ash-based geopolymer concrete beams* (pp. 11–14). Newcastle: Proceedings of Australian Structural Engineering, Conference.

Thakkar, S., Dave, U., & Bhatol, D. (2022). Behaviour of ambient cured prestressed and non-prestressed geopolymer concrete beams. *Case Studies in Construction Materials*. https://doi.org/10.1016/j.cscm.2021.e00798

Walkley, B., Rees, G., SanNicolas, R., vanDeventer, J., Hanna, J., & Provis, J. (2018). New structural model of sodium aluminosilicate gels and the role of charge balancing extra-framework Al. *Journal of Physical Chemistry C, 122*, 5673–5685. https://doi.org/10.1021/acs.jpcc.8b00259

Wanchai, Y. (2014). Application of fly ash-based geopolymer for structural member and repair materials. *Advances in Science and Technology, 92*, 74–83. https://doi.org/10.4028/www.scientific.net/AST.92.74

Wu, Y., Xie, S., Zhang, Y., Du, F., & Cheng, C. (2018). Super high strength of geopolymer with the addition of polyphosphate. *Ceramics International, 44*, 2578–2583. https://doi.org/10.1016/j.ceramint.2017.11.020

Yost, J., Radlinska, A., Ernst, S., Salera, M., & Martignetti, N. (2013). Structural behavior of alkali activated fly ash concrete. Part 2: structural testing and experimental findings. *Materials and Structures, 46*, 449–462. https://doi.org/10.1617/s11527-012-9985-0

Publisher's Note